

# Overview of NICMOS

## In this chapter . . .

2.1 Instrument Capabilities / 13
2.2 Heating, Cooling and Focus / 15
2.3 NICMOS Instrument Design / 16
2.4 Basic Operations / 21

---

## 2.1 Instrument Capabilities

NICMOS, the Near Infrared Camera and Multi-Object Spectrometer, is an HST axial instrument, containing three cameras designed for simultaneous operation. The NICMOS optics offer three adjacent but not spatially contiguous fields-of-view of different image scales. The instrument covers the wavelength range from 0.8 to 2.5 microns, and contains a variety of filters, grisms, and polarizers. Each camera carries a complement of 19 optical elements, selected through independent filter wheel mechanisms, one per camera. In order to allow operation of the NICMOS detectors and to minimize the thermal background of the instrument, NICMOS needs to be cooled to cryogenic temperatures. The basic capabilities of the instrument are presented in Table 2.1.

**IR imaging:** NICMOS provides its highest sensitivity from 1.1 to ~2 microns, where it is superior to an 8m class telescope. Chapter 4 discusses the overall throughput of NICMOS and the optical elements available in each camera. The low background which HST offers between 0.8 and 2 microns allows deep photometry. Our estimates of limiting sensitivities per pixel for a  $5\sigma$  detection in a 3,600 second integration, at an operating temperature of 77.15K, are given in Table 2.2. Users should note that an integration time of 3600 sec is not practical and is for illustrative purposes.

Table 2.1: Overview NICMOS Capabilities

Mode	NIC1	NIC2	NIC3	Comments
<b>Imaging</b>				
• FOV (arcsec)	11×11	19.2×19.2	51.2×51.2	
• Scale (arcsec/pixel)	0.043	0.075	0.2	
• Sensitivity limit (J, H, K) <sup>a</sup>	25.2,23.7,—	26.3,24.8,20.1	26.5,25.6,20.7	S/N = 5, t <sub>exp</sub> = 3600 s
• Diffraction limit (μm)	1.0	1.75	—	
<b>Grism Spectroscopy</b>				
• Type			MOS slitless	
• R			200	per pixel
• Δλ (μm)			0.8–1.2	G096
			1.1–1.9	G141
			1.4–2.5	G206
• Magnitude limit (Vega H-band) <sup>a</sup>			20.5,20.4,16.6	A0V, S/N=5, t <sub>exp</sub> = 3600 s
<b>Polarimetry</b>				
• Filter angles (deg)	0, 120, 240	0, 120, 240		
• Δλ (μm)	0.8–1.3	1.9–2.1		
<b>Coronagraphy</b>				
• hole radius (arcsec)		0.3		cold mask

a. Limiting magnitudes are from the NICMOS ETC (see Chapter 9). Infrared passbands (J,H,K) are defined by Bessell and Brett (1988, PASP, 100, 1134).

- **Grism Spectroscopy:** Camera 3 has three gratings which provide a multi-object spectroscopic capability with a resolving power of R~200 per pixel over the full field of view of the camera. Their wavelength ranges are 0.8 to 1.2 microns, 1.1 to 1.9 microns, and 1.4 to 2.5 microns. Because the gratings are slitless, the spectra of spatially resolved objects are confused and multiple objects can overlap.
- **Imaging Polarimetry:** Three polarizing filters with pass directions of 0, 120, and 240 degrees are provided for the wavebands 0.8–1.2 microns in Camera 1 and 1.9–2.1 microns in Camera 2.

- **Coronagraphy:** A 0.3 arcsec radius occulting hole and cold mask, in the intermediate resolution Camera 2, provide a coronagraphic imaging capability.

Chapter 5 discusses these three special capabilities in more detail.

Table 2.2: Limiting Sensitivities in Janskys for S/N = 5 detection of a point source in a standard aperture of diameter 0.5", 0.5", and 1" for NIC1, NIC2, and NIC3, respectively, for a 3600 sec exposure.<sup>a,b</sup>

Camera	Filter	Bandwidth (microns)	Limiting Sensitivity	
			Jansky	Approx. Mag.
NIC1	F110W	0.8–1.35	$1.75 \times 10^{-7}$	J $\approx$ 25.2
NIC1	F160W	1.4–1.8	$6.26 \times 10^{-7}$	H $\approx$ 23.7
NIC2	F110W	0.8–1.35	$6.73 \times 10^{-8}$	J $\approx$ 26.3
NIC2	F160W	1.4–1.8	$2.21 \times 10^{-7}$	H $\approx$ 24.8
NIC2	F237M	2.3–2.5	$1.71 \times 10^{-5}$	K $\approx$ 20.1
NIC3	F110W	0.8–1.35	$5.49 \times 10^{-8}$	J $\approx$ 26.5
NIC3	F160W	1.4–1.8	$4.75 \times 10^{-8}$	H $\approx$ 25.6
NIC3	F240M	2.3–2.5	$9.83 \times 10^{-6}$	K $\approx$ 20.7

a. S/N calculated for brightest pixel in point source image, using the NICMOS ETC for 77.15K temperature.

b. Limiting magnitudes are from the NICMOS ETC (Chapter 9). Infrared passbands (J,H,K) are defined by Bessell and Brett (1988, PASP, 100, 1134). A0V spectrum assumed to convert between NICMOS passband flux (in Jy) and conventional, Vega-normalized JHK magnitudes.

## 2.2 Heating, Cooling and Focus

After NICMOS was installed in HST, the dewar was planned to warm up to about 57 K, a temperature never reached during ground testing. The ice expansion caused by this temperature increase resulted in an additional dewar deformation, to the extent that one of the (cold) optical baffles made mechanical contact with the vapor-cooled shield (VCS). The resulting heat flow caused the ice to warm up beyond expectations, to about 60 K, which in turn deformed the dewar more. The motion history of NICMOS and the resulting image quality are discussed in Chapter 4 and a more detailed history of the dewar distortion can be found at:

<http://www.stsci.edu/hst/nicmos/design/history>

This unexpectedly large deformation had several undesirable effects, the most important of which are:

- The three cameras have significantly different foci, hence parallel observations are degraded. The difference between the NIC1 and NIC2 foci, however, is sufficiently small that an intermediate focus yields good quality images in both cameras.
- The NIC3 focus has moved outside of the range of the PAM. In an attempt to bring it to within the focus range, the secondary mirror was moved during two brief NIC3 campaigns in Cycle 7. During this time, HST performed exclusively NIC3 science, since no other HST instrument was in focus. Because of the extreme impact on all other instruments, no such campaigns are planned in the future. At the maximum PAM position, the degradation in terms of encircled energy at a 0.2" radius is only 5%. This is considered sufficiently small, and NIC3 will be offered "as is" in Cycle 11 and beyond.

The thermal short increased the heat flux into the inner shell (and therefore the solid nitrogen) by a factor of 2.5 and thereby reduced the lifetime of NICMOS from 4.5 to ~2 years. The cryogen depleted in January 1999, and NICMOS was unavailable for science operation between January 1999 and June 2002, when the NICMOS cooling system was activated and reached expected operating temperatures.




---

*The installation of the NICMOS Cooling System (NCS), a mechanical cryocooler re-enabled NICMOS operation, and restored infrared capability to HST. The NCS is capable of cooling the NICMOS dewar to temperatures 75–86 K, significantly higher than during Cycle 7. So far, the temperature control is good enough to keep the detector temperature to 77.15 ± 0.10 K. Therefore, many NICMOS parameters are different from Cycle 7. Most notably the detector quantum efficiency (DQE) increased by ~30–50%.*

---

## 2.3 NICMOS Instrument Design

### 2.3.1 Physical Layout

NICMOS is an axial bay instrument which replaced the Faint Object Spectrograph (FOS) in the HST aft shroud during the Second HST Servicing Mission in February 1997. Its enclosure contains four major elements: a graphite epoxy bench, the dewar, the fore-optics bench, and the electronics boxes. The large bench serves to establish the alignment and dimensional stability between the HST optics (via the latches or fittings),

the room temperature fore optics bench, and the cryogenic optics and detectors mounted inside the dewar. The NICMOS dewar was designed to use solid nitrogen as a cryogen for a design lifetime of approximately  $4.5 \pm 0.5$  years. Cold gas vented from the dewar was used to cool the vapor cooled shield (VCS) which provides a cold environment for both the dewar and the transmissive optical elements (i.e., the filters, polarizers, and grisms). The VCS is itself enclosed within two layers of thermal-electrically cooled shells (TECs).

Figure 2.1 is an overview of the NICMOS instrument; Figure 2.2 shows details of the dewar. The external plumbing at the dewar aft end, which was used for the periodical recooling of the solid nitrogen during ground testing, now forms the interface to the NCS. During SM3B, the NCS was connected to the bayonet fittings of the NICMOS interface plate. This allows the NCS to circulate cryogenic Neon gas through the cooling coils in the dewar, thus providing the cooling power to bring the instrument into the temperature range required for operation. The concept and working principles of the NCS are discussed in Appendix E.

Figure 2.1: Instrument Overview

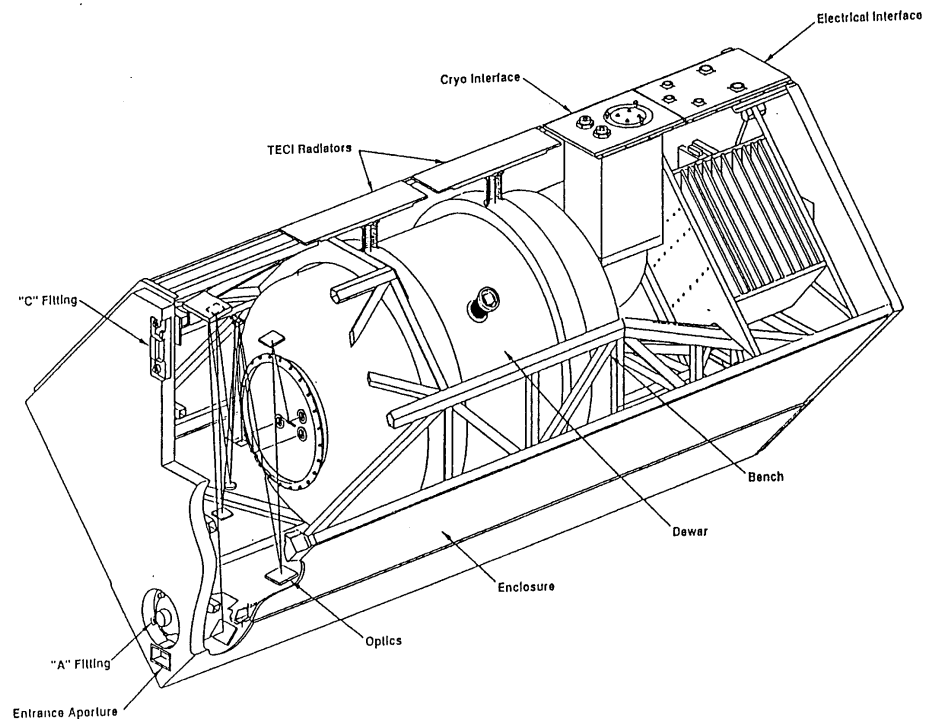
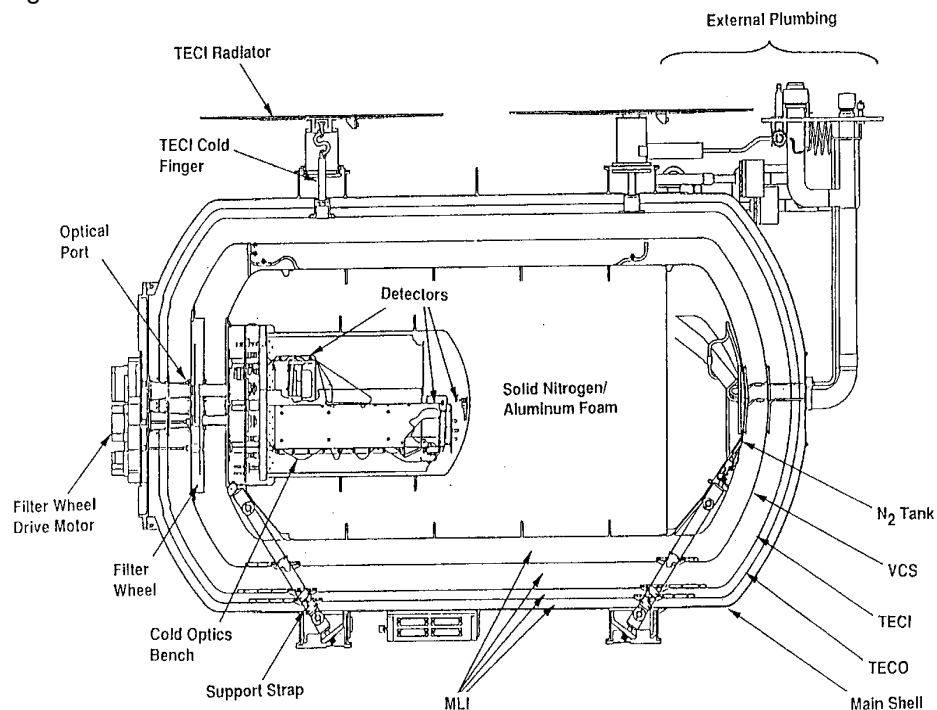


Figure 2.2: NICMOS Dewar



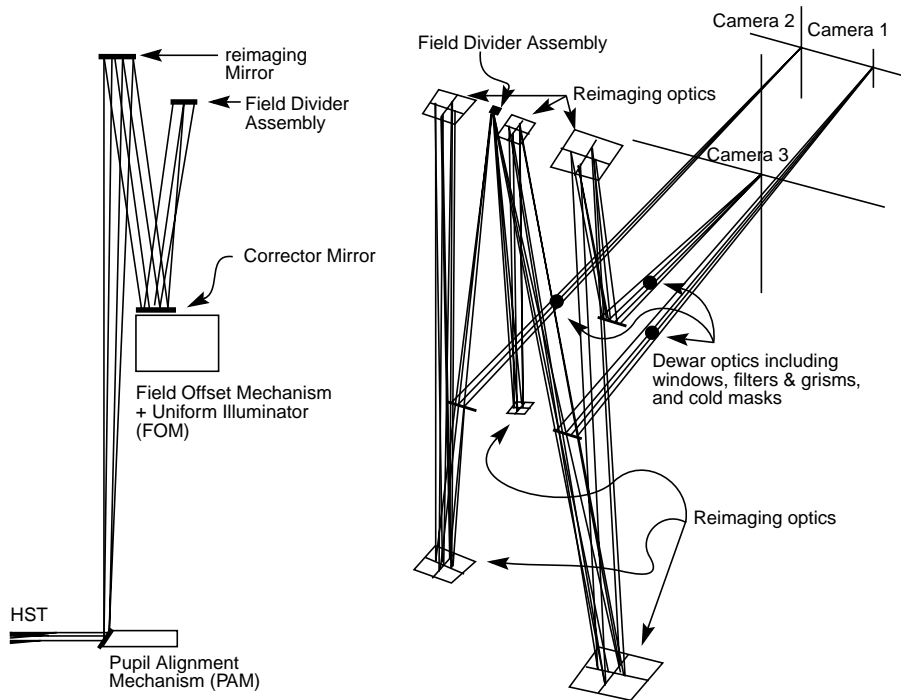
### 2.3.2 Imaging Layout

The NICMOS fore-optics assembly is designed to correct the spherically aberrated HST input beam. As shown in the left hand panel of Figure 2.3 it comprises a number of distinct elements. The Pupil Alignment Mechanism (PAM) directs light from the telescope onto a re-imaging mirror, which focuses an image of the Optical Telescope Assembly (OTA) pupil onto an internal Field-Offset Mechanism (FOM) with a pupil mirror that provides a small offset capability (26 arcsec). An internal flat field source is also included in the FOM assembly. In addition, the FOM provides correction for conic error in the OTA pupil.

After the FOM, the Field Divider Assembly (FDA) provides three separate but closely-spaced imaging fields, one for each camera (right hand panel of Figure 2.3). The dewar itself contains a series of cold masks to eliminate stray IR emission from peripheral warm surfaces.

A series of relay mirrors generate different focal lengths and magnifications for the three cameras, each of which contains a dedicated  $256 \times 256$  pixel HgCdTe chip that is developed from the NICMOS 3 detector design. NICMOS achieves diffraction limited performance in the high resolution NIC1 longward of 1.0 microns, and in NIC2 longward of 1.75 microns.

Figure 2.3: Ray Diagrams of the NICMOS Optical Train. The left panel shows the fore-optics. The right panel shows the field divider and re-imaging optics for the three cameras.



The operation of each camera is separate from the others which means that filters, integration times, readout times and readout modes can be different in each, even when two or three are used simultaneously. The basic imaging properties of each of the cameras are summarized in Table 2.3.

Table 2.3: Basic Imaging Parameters

Parameter	Camera 1	Camera 2	Camera 3
Pixel Size (arcsec)	0.043	0.075	0.2
Field of View (arcsec x arcsec)	11 × 11	19.2 × 19.2	51.2 × 51.2
<i>f</i> ratio	<i>f</i> /80	<i>f</i> /45.7	<i>f</i> /17.2
Diffraction Limited Wavelength (μm)	1.0	1.75	—

### 2.3.3 Camera NIC1

NIC1 offers the highest available spatial resolution with an 11 × 11 arcsec field of view and 43 milliarcsec sized pixels (equivalent to the WFPC2 PC pixel scale). The filter complement includes broad and medium band filters covering the spectral range from 0.8 to 1.8 microns and narrow

band filters for Paschen  $\alpha$ , He I, [Fe II]  $\lambda$  1.64 $\mu$ m, and [S III]  $\lambda$  0.953  $\mu$ m, both on and off band. It is equipped with the short wavelength polarizers (0.8 to 1.3 microns).

### 2.3.4 Camera NIC2

NIC2 provides an intermediate spatial resolution with a  $19.2 \times 19.2$  arcsec field of view and 75 milliarcsec pixels. The filters include broad and medium band filters covering the spectral range from 0.8 to 2.45 microns. The filter set also includes filters for CO, Brackett  $\gamma$ , H<sub>2</sub> S2 (1-0)  $\lambda$  2.122  $\mu$ m, Paschen  $\alpha$ , HCO<sub>2</sub> + C<sub>2</sub>, and the long wavelength polarizers (1.9–2.1 microns). Camera 2 also provides a coronagraphic hole with a 0.3 arcsec radius.

### 2.3.5 Camera NIC3

NIC3 has the lowest spatial resolution with a large  $51.2 \times 51.2$  arcsec field of view and 200 milliarcsec pixels. It includes broad band filters covering the spectral range 0.8 to 2.3 microns, medium band filters for the CO band (and an adjacent shorter wavelength continuum region), and narrow band filters for H<sub>2</sub> S2 (1-0), [Si VI]  $\lambda$  1.962  $\mu$ m, Paschen- $\alpha$ , [Fe II]  $\lambda$  1.64  $\mu$ m, and He I  $\lambda$  1.083  $\mu$ m. Camera 3 also contains the multi-object spectroscopic capability of NICMOS with gratings covering the wavelength ranges 0.8–1.2 microns, 1.1–1.9 microns, and 1.4–2.5 microns.

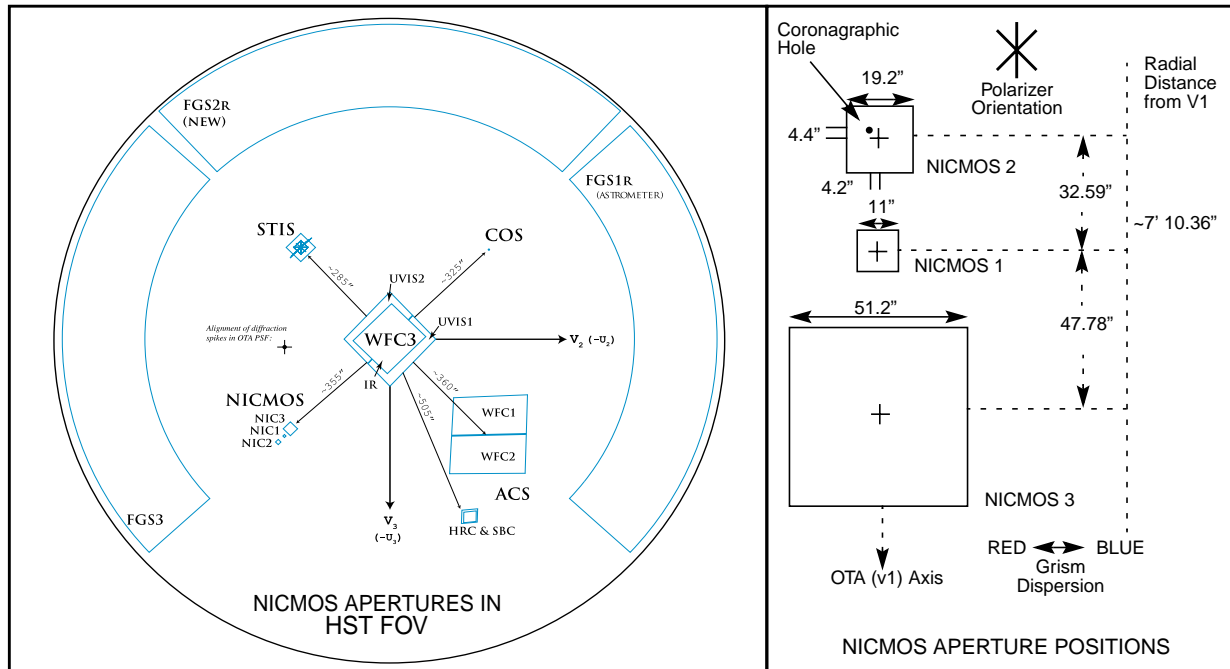
### 2.3.6 Location and Orientation of Cameras

The placement and orientation of the NICMOS cameras in the HST focal plane is shown in Figure 2.4. Notice that the cameras are in a straight line pointing radially outward from the center of the telescope focal plane. From the observer's point of view the layout of NICMOS is most relevant when trying to plan an observation of an extended source with all three cameras simultaneously. The user must then bear in mind the relative positions and orientations of the three cameras. The gaps between the cameras are large, and therefore getting good positioning for all cameras may be rather difficult.

The position of the NICMOS cameras relative to the HST focal plane (i.e., the FGS frame) depends strongly on the focus position of the PAM. Since independent foci and their associated astrometric solutions are supported for each camera, this is transparent to the observer. However, the relative positions of the NICMOS cameras in the focal plane could affect the planning of coordinated parallels with other instruments.



Figure 2.4: NICMOS Field Arrangement



## 2.4 Basic Operations

In this section, we give a brief description of the basic operations of each NICMOS detector (see Chapter 7 for more details), and compare the infrared arrays to CCDs. We then discuss the target acquisition modes for coronagraphy (see Chapter 5 for a more extensive description of coronagraphy), as well as the simultaneous use of NIC1 and NIC2.

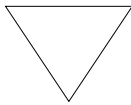
### 2.4.1 Detectors' Characteristics and Operations

NICMOS employs three low-noise, high QE, 256×256 pixel HgCdTe arrays. Active cooling provided by the NCS keeps the detectors' temperature at ~77.15 K. The detector design is based on the NICMOS3-type design, described in more detail in Chapter 7. Here we summarize the basic properties of the NICMOS detectors most relevant to the planning of observations.

The NICMOS detectors have dark current of about 0.1–0.2 electrons per second and the effective readout noise for a single exposure is approximately 30 electrons.

The NICMOS detectors are capable of very high dynamic range observations and have no count rate limitations in terms of detector safety. The dynamic range, for a single exposure, is limited by the depth of the full

well, or more correctly by the onset of strong non-linearity, which limits the total number of electrons which can be accumulated in any individual pixel during an exposure. Unlike CCDs, NICMOS detectors do not have a linear regime for the accumulated signal; the low- and intermediate-count regime can be described by a quadratic curve and deviations from this quadratic behavior is what we define as ‘strong non-linearity’. Current estimates under NCS operations give a value of ~120,000 electrons (NIC1 and NIC2) or 155,000 electrons (NIC3) for the 5% deviation from quadratic non-linearity.

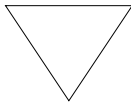



---

***There are no bright object limitations for the NICMOS detectors. However, one must consider the persistence effect. See Section 4.6 Photon and Cosmic Ray Persistence for details.***

---

NICMOS has three detector read-out modes that may be used to take data (see Chapter 8) plus a target acquisition mode (ACCUM, MULTIACCUM, BRIGHTOBJ, and ACQ).




---

***Only ACCUM, MULTIACCUM, and ACQ are supported in Cycle 11 and beyond and ACCUM mode observations are strongly discouraged.***

---

The simplest read-out mode is ACCUM which provides a single integration on a source. A second mode, called MULTIACCUM, provides intermediate read-outs during an integration that subsequently can be analyzed on the ground. A third mode, BRIGHTOBJ, has been designed to observe very bright targets that would otherwise saturate the detector. BRIGHTOBJ mode reads-out a single pixel at a time. Due to the many resets and reads required to map the array there are substantial time penalties involved. BRIGHTOBJ mode may not be used in parallel with the other NICMOS detectors. BRIGHTOBJ mode appears to have significant linearity problems and has not been tested, characterized, or calibrated on-orbit.

Users who require time-resolved images will have to use MULTIACCUM where the shortest spacing between non-destructive exposures is 0.203 seconds.

MULTIACCUM *mode should be used for most observations.* It provides the best dynamic range and correction for cosmic rays, since post-observation processing of the data can make full use of the multiple readouts of the accumulating image on the detector. Exposures longer than about 10 minutes should always opt for the MULTIACCUM read-out mode, because of the potentially large impact of cosmic rays. To enhance the utility of MULTIACCUM mode and to simplify the implementation,

execution, and calibration of MULTIACCUM observations, a set of MULTIACCUM sequences has been pre-defined (see Chapter 8). The observer, when filling out the Phase II proposal, needs only to specify the name of the sequence and the number of samples which should be obtained (which defines the total duration of the exposure).

## 2.4.2 Comparison to CCDs

These arrays, while they share some of the same properties as CCDs, are not CCDs and offer their own set of advantages and difficulties. Users unfamiliar with IR arrays should therefore not fall into the trap of treating them like CCDs. For convenience we summarize the main points of comparison:

- As with CCDs, there is read-noise (time-independent) and dark current noise (time-dependent) associated with the process of reading out the detector. The dark current associated with NICMOS arrays is quite substantial compared to that produced by the current generation of CCDs. In addition, there is an effect called *shading* which is a time-variable bias from the last read affecting the readout amplifiers.
- Unlike a CCD, the individual pixels of the NICMOS arrays are strictly independent and can be read non-destructively. Read-out modes have been designed which take advantage of the non-destructive read capabilities of the detectors to yield the optimum signal-to-noise for science observations (see Chapter 7, 8). Because the array elements are independently addressed, the NICMOS arrays do not suffer from some of the artifacts which afflict CCDs, such as charge transfer smearing and *bleeding* due to filling the wells. If, however, they are illuminated to saturation for sustained periods they retain a *memory (persistence)* of the object in the saturated pixels. This is only a concern for the photometric integrity of back to back exposures of very bright targets, as the ghost images take many minutes, up to one hour, to be flushed from the detectors.

## 2.4.3 Target Acquisition Modes

Most target acquisitions can be accomplished by direct pointing of the telescope. The user should use the Guide Star Catalog-II to ensure accurate target coordinates. Particular care must be exercised with targets in NIC1 due to its small field of view.

However, direct pointing will not be sufficient for coronagraphic observations since the achieved precision ( $1\sigma = 0.33''$ ) is comparable to the size of the coronagraphic spot ( $0.3''$ ). *Note that this is the HST pointing*

*error only. Possible uncertainties in the target coordinates need to be added to the total uncertainty.*

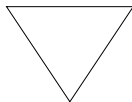
There are three target acquisition options for coronagraphic observations, which are extensively discussed in Chapter 5:

- On-board acquisition (Mode-2 Acquisition). This commands NICMOS to obtain an image of the target and rapidly position the brightest source in a restricted field of view behind the coronagraphic hole. This is one of the pre-defined acquisition modes in the Phase II proposals (ACQ mode).
- The RE-USE TARGET OFFSET special requirement can be used to accomplish a positioning relative to an early acquisition image.
- A real time acquisition (INT-ACQ) can be obtained, although this is costly in spacecraft time and is a limited resource.

While ACQ mode is restricted to coronagraphic observations in Camera 2, the last two target acquisition modes may be useful for positioning targets where higher than normal (1–2 arcsec) accuracy is required (e.g., crowded field grism exposures).

#### 2.4.4 Attached Parallels

While the three NICMOS cameras are no longer at a common focus, under many circumstances it is desirable to obtain data simultaneously in multiple cameras.




---

*The foci of Cameras 1 and 2 are close enough that they can be used simultaneously, whereas Camera 3 should be used by itself.*

---

Although some programs by their nature do not require more than one camera (e.g., studies of isolated compact objects), observers may nonetheless add exposures from the other camera to their proposals in order to obtain the maximum amount of NICMOS data consistent with efficiently accomplishing their primary science program. Internal NICMOS parallel observations obtained together with primary science observations will be known as *coordinated parallels* and will be delivered to the prime program's observer and will have the usual proprietary period.